View metadata, citation and similar papers at core.ac.uk

brought to you by CORE

provided by IntechOpen

We are IntechOpen, the world's leading publisher of Open Access books Built by scientists, for scientists

4,800
Open access books available

122,000
International authors and editors

135M
Downloads

Our authors are among the

154
Countries delivered to

TOP 1%
most cited scientists

12.2%
Contributors from top 500 universities

CLARIVATE ANALYTICS BOOK CITATION INDEX INDEXED

WEB OF SCIENCE™

Selection of our books indexed in the Book Citation Index in Web of Science™ Core Collection (BKCI)

Interested in publishing with us?
Contact book.department@intechopen.com

Numbers displayed above are based on latest data collected.
For more information visit www.intechopen.com

27

Three Dimensional Nanoimprint Lithography using Inorganic Electron Beam Resist

Jun Taniguchi and Noriyuki Unno
Tokyo University of Science
Japan

1. Introduction

With the advancement in the information technology the need for increasingly complex three-dimensional (3D) structure is eminent. Gray scale lithography can produce 3D structure but it cannot match the resolution of electron beam lithography (EBL). Today the EBL is primarily used for mask making and for making nanoimprint lithography (NIL) molds (Chou *et al.*, 1995), but these structures do not require features with varying depths. Hence EB systems under their current mode of operation cannot build 3D nanostructures. Typically, EB systems are operated at high accelerating voltage (>50 kV) with beam diameter capable of writing at nano-scale (Ishii & Matsuda, 1992). However, high kV EB because of its poor interaction with resist causes poor resist sensitivity resulting in low throughput. It is also difficult to control depth because dose change affects EB blur resulting in feature width spread during develop. This problem can be resolved at low kV operation where increased EB/resist interaction improves resist sensitivity (Olkhovets & Craighead, 1999). Inorganic resist is transparent, so it can be directly applied to an optical surface. Since the transparency of this type of resist extends to ultraviolet (UV) light, it can also be used for making UV-NIL mold. Using the resist we fabricated 3D mold by controlling the acceleration voltage, and then we replicated the mold with nano-order patterns by using UV-NIL. Usually, fabrication of binary optics element involving repeated overlays and dry etch results in poor resolution and is expensive. However, control of acceleration voltage electron beam lithography (CAV-EBL) can fabricate binary optics element by using only EB, and thus makes the process cost effective. Hence fabrication of 3D NIL mold using CAV-EBL is described.
Furthermore, the method of improving the resolution and the contrast using post exposure bake (PEB) with inorganic resist is also described. Although no chemically amplified material is contained in our inorganic resist, PEB was characteristically applied in our process. PEB process causes the anneal effect for inorganic resist and the proximity effect is suppressed, resulting in high contrast.

2. Three dimensional nanoimprint lithography

2.1 Experimental apparatus and procedures

At first, Accuglass-512B, a Spin-on-Glass (SOG) composed mainly of siloxane with 14% organic content whose interlayer dielectrics were developed by Honeywell Co., was used

Source: Lithography, Book edited by: Michael Wang,
ISBN 978-953-307-064-3, pp. 656, February 2010, INTECH, Croatia, downloaded from SCIYO.COM

for inorganic resist. The structure is shown in Fig. 1. A buffered hydrofluoric acid (BHF) solution (50%, HF 25 cm^3/l, and 40% NH_4F 30 cm^3/l) was used for developer. The calculated concentration of [HF] was 0.43 mol/l and that of [HF_2^-] was 0.29 mol/l. ERA-8800FE (ELIONIX Co.) was used for EB system with several pA of beam current and about 10 nm beam diameter. The fabrication process of 3D mold involved three steps (Fig. 2). At first, SOG was spin-coated on a Si substrate and cured at 425 ^oC for 1 h resulting in a 450 nm film. Then the sample was written with EB with uniform doses at different acceleration voltages. In the case of the CAV-EBL, the developed depth was controlled by varying the voltage to change the electron range where low and high voltages gave shallow and deep pits. Then the EB-exposed SOG was developed out with BHF solution in 60 s but it did not

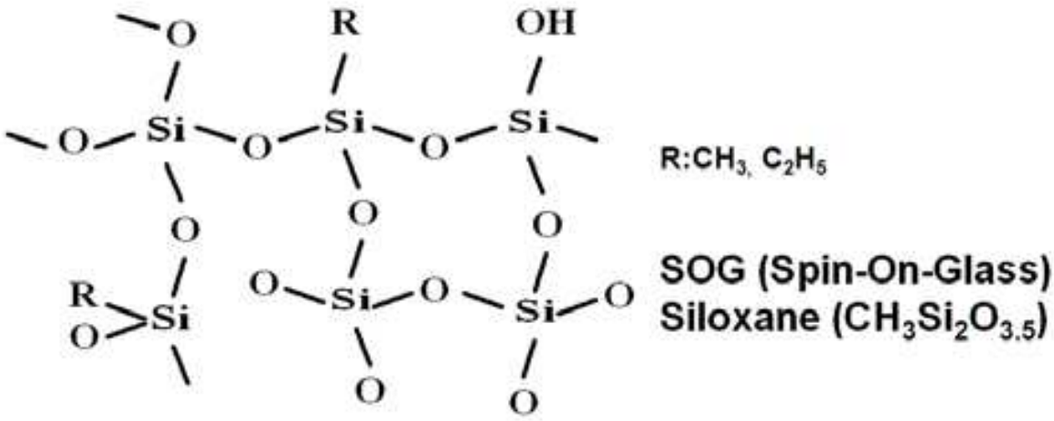

Fig. 1. The structure of spin-on-glass inorganic resist.

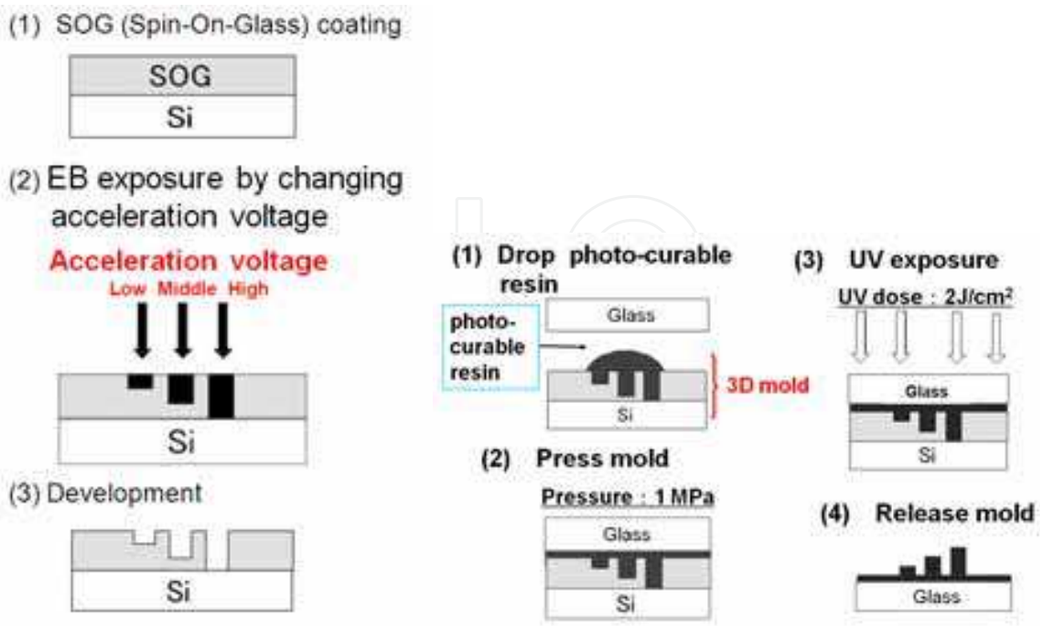

(a) (b)

Fig. 2. Process for (a)fabrication of 3D mold with CAV-EBL and (b)UV-NIL.

etch EB-unexposed SOG within 60 s which was helpful in fabricating molds with different depth gradations. For this experiment we used a house-made UV-NIL machine equipped with a UV light source SP-6 (USIO Co.). The process was as follows: at first, a fabricated 3D mold was coated with anti-sticking layer Optool DSX (DAIKIN INDUSTRIES, LTD). Then, a UV photo-curable resin PAK01 (made by Toyo Gosei Co., Ltd.) was dispensed onto a quartz substrate. Next, the mold was pressed against the resin film on the substrate with 1 MPa for 60 s. The photo-curable resin was then exposed to a 2 J/cm^2 dose of UV light through the quartz substrate. The mold was then retracted leaving behind a 3D replica of its pattern. To make the precise measurement of depth dependence on acceleration voltage change, we used a step profilometer (KLA-Tencor alpha-step 500). To enable the profilometer stylus to reach to the bottom of the patterns, we set the drawing pattern width to 10 µm. The mold and replicated pattern was observed with atomic force microscope (SII 100 SPA-400), and scanning electron microscope (SEM, ELIONIX, ERA-8800FE) was used to examine the pattern. The cross-sections of lines were observed with SEM by tilting the specimen to 75◦.

2.2 3D UV-NIL

To evaluate the EB dose effect in the CAV-EBL, the acceleration voltage was varied from 1 to 4 kV by 30 V increments. In this case, each accelerating voltage was exposed at 200 and 500 µC/cm^2 dose. The designed line-width for this evaluation was 10 µm. Fig. 3 shows the relationship between acceleration voltage and developed depth. This figure mean that the effect of EB dose on the developed depths was quite noticeable at higher accelerating voltage. In contrast, in low acceleration voltage region (< 2kV) there was no effect of dose change on developed-depth. Thus, in order to control the develop depths, controlling the dose is important. Furthermore, a 5 nm depth control is possible using CAV-EBL and spin on glass as an EB resist.

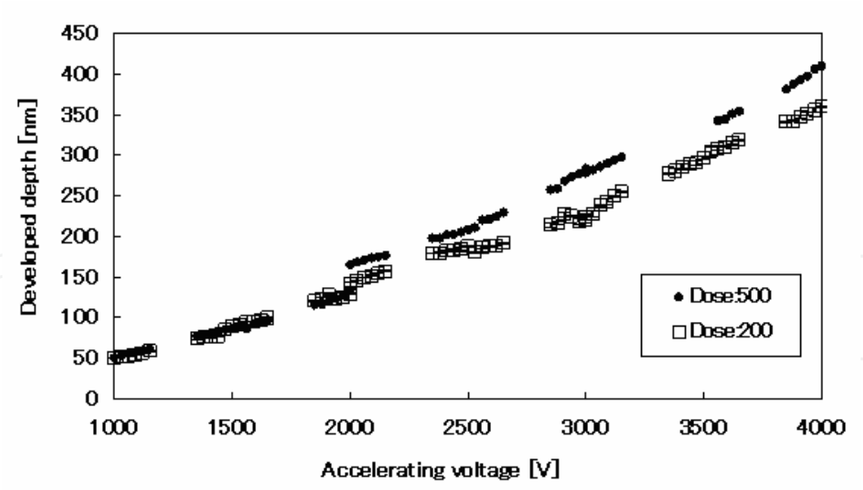

Fig. 3. The relationship between acceleration voltage and developed depth.

Next, we fabricated a blade-shaped mold for binary optics by superposition of different depth areas using stepping motors on SEM stage. However, these motors had limited accuracy of around 500 nm, so superposition of areas width needed to be wider than 500 nm and hence a designed line-width of 2 µm was chosen. Control of depths was carried out by changing the accelerating voltage where seven stairs were formed by using 2, 2.5, 3, 3.5, 4,

4.5 and 5 kV accelerating voltage. For each stair the EB dose was set at 250 μC/cm². Fig. 4 shows AFM images of 3D mold where seven stairs were obtained.

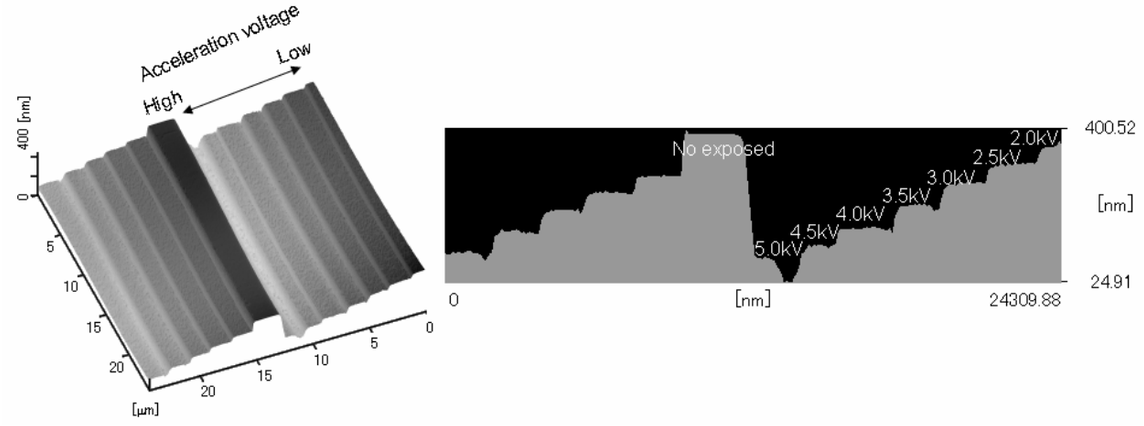

Fig. 4. The AFM images of 3D mold where seven stairs.

Using this mold, UV-NIL was carried out. Fig. 5 shows replicated patterns on photo-curable resin, and table I shows developed-depths of mold and heights of UV-NIL patterns. The mold depths were corresponded to the replicated heights. Hence, volume production of binary optics elements is possible by using CAV-EBL and UV-NIL. The developed depths in table I also agree with the values in Fig. 3.

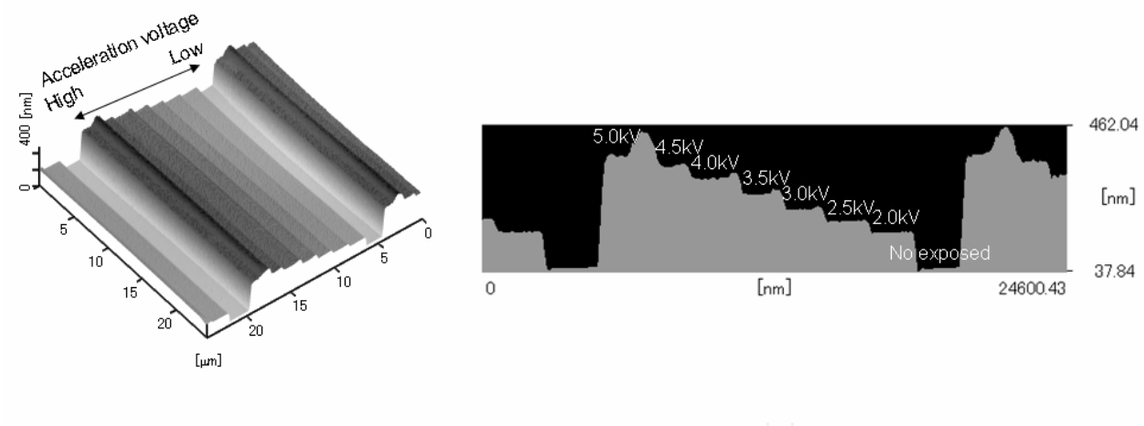

Fig. 5. The AFM images of replicated patterns on photo-curable resin.

Fig. 6 shows a sub-100 nm 3D nanoimprint mold and the UV-NIL pattern on photo-curable resin that we obtained, similar to a blade-shaped mold. The transfer pressure was 3.0 MPa. This result means that the pattern depth can be modulated by using CAV-EBL even at the sub-100 nm scale. The replicated heights were shorter than mold depths, because the photo-curable resin was shrunk by curing at UV exposure. However, the mold line-widths and the replicated pattern line-widths matched, and the replicated pattern heights were also modulated. Thus, the realization of sub-100 nm 3D mold fabrication was possible using CAV-EBL.

Accelerating Voltage [kV]	Depth of stair in 3D mold [nm]	Height of replicated pattern [nm]
2	100.2	106.9
2.5	136.4	143.6
3	173.1	178.4
3.5	220.7	221.9
4	261.6	265.9
4.5	305.3	304.2
5	328.2	325.8

Table I. 3D mold depths and 3D replicated height.

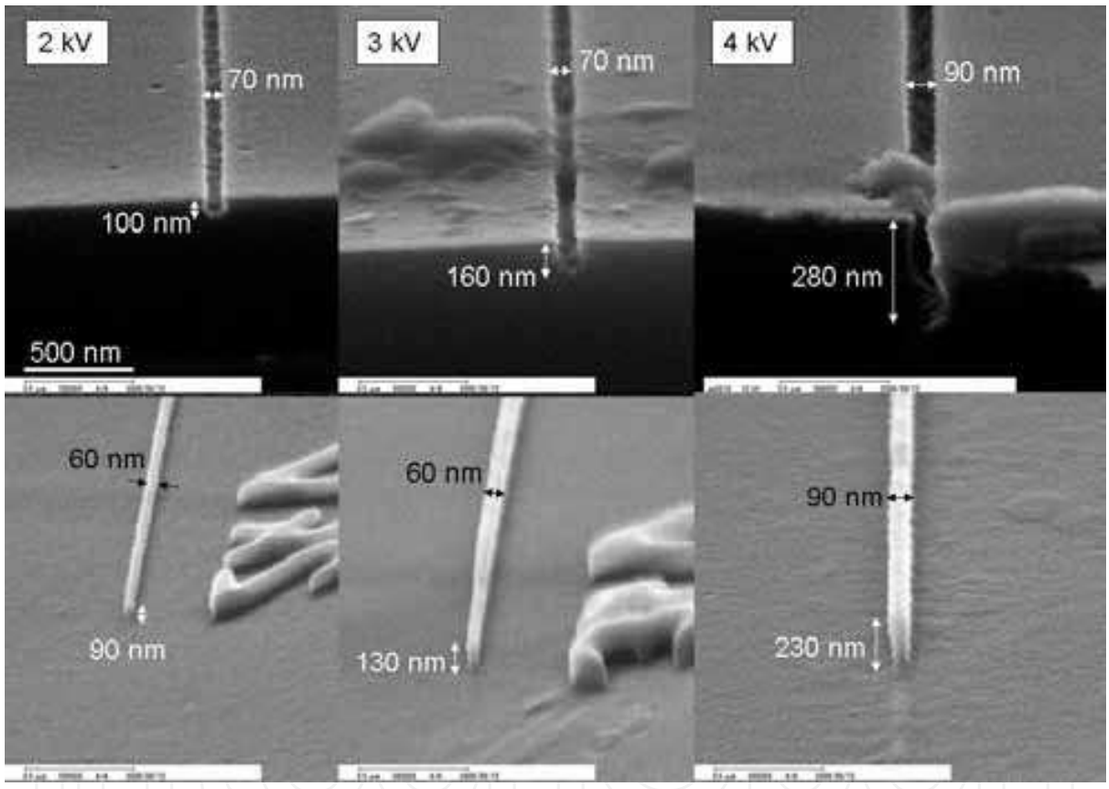

Fig. 6. The fabricated sub-100 nm 3D nanoimprint mold and the UV-NIL pattern

3. Improving the inorganic resist

We used a Spin-On-Glass (SOG) material, Accuglass 512B (Honeywell Co. Ltd.), for positive EB resist that exhibits low sensitivity and LER. On the other hand, negative EB inorganic resist has high sensitivity and resolution (Namatsu, 2001). Hence, positive EB inorganic resists with high sensitivity and resolution, and low line edge roughness (LER) are now required for low kV EBL. Therefore, an inorganic resist known as Nano Imprint Mold Oxide-Positive tone 0701 (NIMO-P0701) made by TOKYO OHKA KOGYO CO., LTD, was developed for improved sensitivity and was employed to investigate the characteristics of EB exposures.

NIMO-P0701 was mainly composed of siloxane and Photo Base Generator (PBG). NIMO-P0701 was spin-coated (pre; 300 rpm (3 s), main; 3000 rpm (10 s)) on silicon substrates. The NIMO-P0701 film was pre-baked at 300 ◦C (90 s), which is the decomposition temperature of PBG, resulting in an approximately 300 nm film thickness. PBG totally changes Si-O-R into Si-O at low pre-bake temperature of 300 °C and accretive to NIMO-P0701 to achieve high sensitivity and delineate pattern at lower pre-bake temperature. The resist films were then exposed using a Scanning Electron Microscope (SEM; ERA-8800FE, ELIONIX), which was customized for the task.

At first, to investigate the mechanism of lithography for NIMO-P0701, Fourier transform infrared (FT-IR) spectroscopy was employed. Fig. 7 shows FT-IR spectra of exposed area of NIMO-P0701 before, and after develop. After develop shows decrease in Peaks of Si-CH_3 and Si-O indicating the area of NIMO-P0701 developed out.

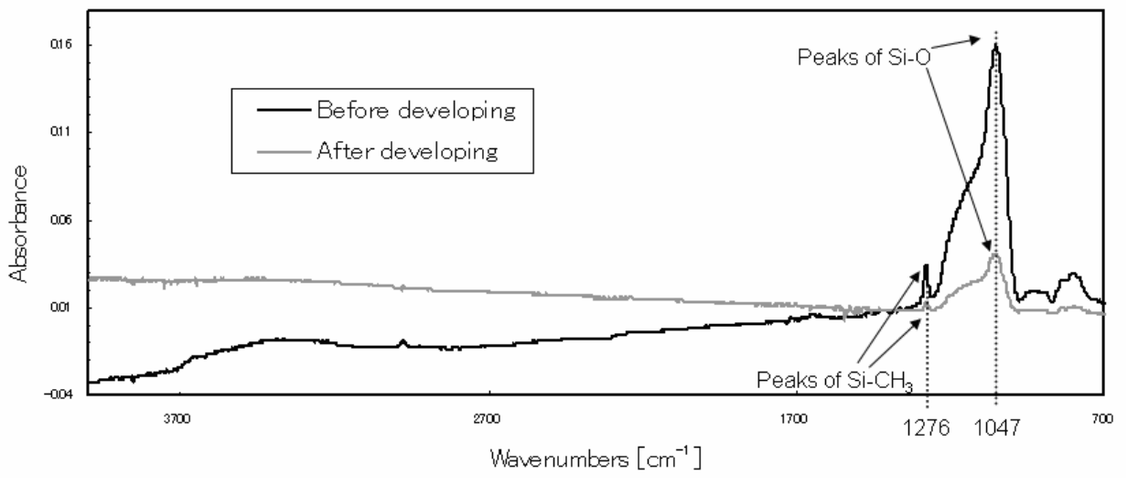

Fig. 7. FT-IR spectra of exposed area of NIMO-P0701 before, and after develop.

Fig. 8 shows FT-IR spectra of exposed and un-exposed areas of NIMO-P0701 after develop. Here the peaks of Si-CH_3 and Si-O in exposed area are significantly lower than the corresponding peaks in the un-exposed area indicating that the exposed area was developed out. The develop mechanism is explained by the conversion of Si-CH_3 into Si-OH when exposed to EB where, unlike Si-CH_3, the newly formed Si-OH is readily soluble in BHF. This behavior results in the appearance of high contrasts.

Next, a developer, buffered hydrofluoric acid (BHF), was optimized. BHF was composed of HF and NH_4F. Mixing ratios and concentrations of these components were varied to optimize the development process. Initially, both resist were developed by 2.4 % concentration BHF (HF:NH_4F=1:1). This concentration has been used for Accuglass 512B. But developing characteristic of NIMO-P0701 turned out to be of low contrast and sensitivity. And hence, the developer for NIMOP0701 had to be optimized. We found that a 2.5% concentration BHF (HF:NH_4F=7:3) was optimum developer for NIMO-P0701. Fig. 9 shows the sensitivity curves of NIMO-P0701 and Accuglass 512B with 4 kV EB. Here NIMO-P0701, developed by 2.5% concentration BHF (HF: NH_4F=7:3), shows higher sensitivity and contrast compared to that of Accuglass 512B.

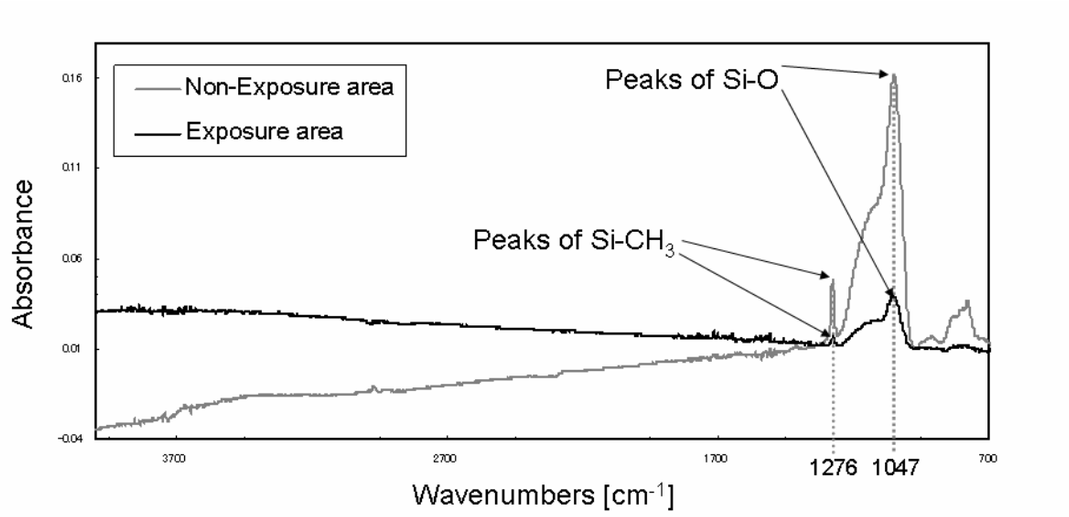

Fig. 8. FT-IR spectra of exposed and un-exposed areas of NIMO-P0701 after develop.

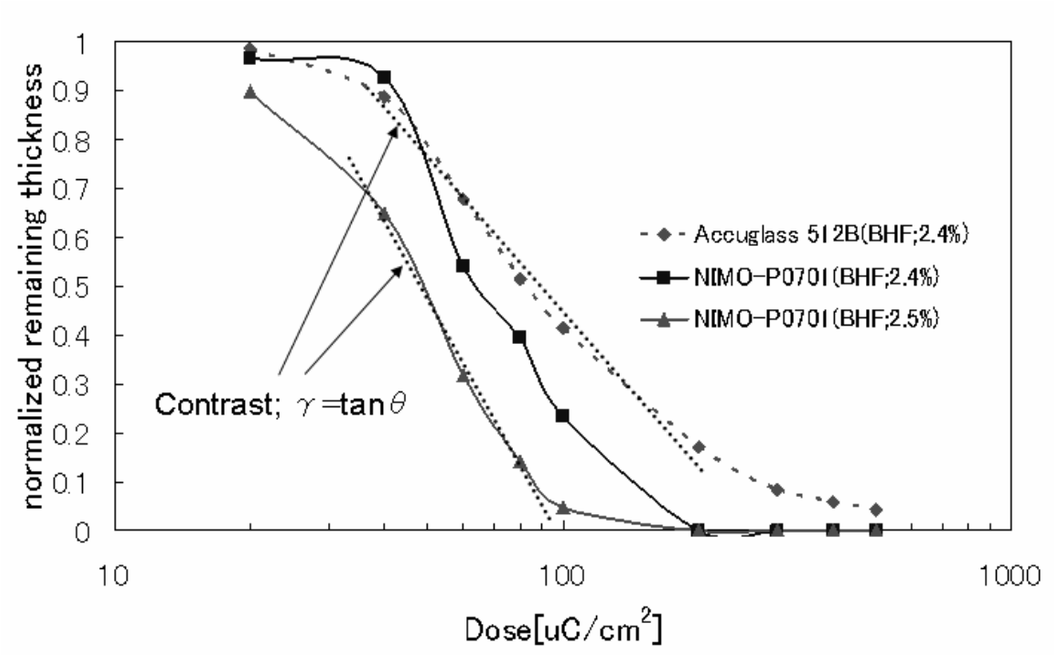

Fig. 9. The sensitivity curves of NIMO-P0701 and Accuglass 512B with 4 kV EB.

Furthermore, the LER was calculated by root-mean-square of line edges which were observed with SEM (Fig. 10). The designed line width is 36nm and space width is 234nm. The condition of EB was 200 μC/cm² at 4 kV. Because of high contrast resulting in high resolution, NIMO-P0701 could be delineated into fine pattern followed by LER measurements.

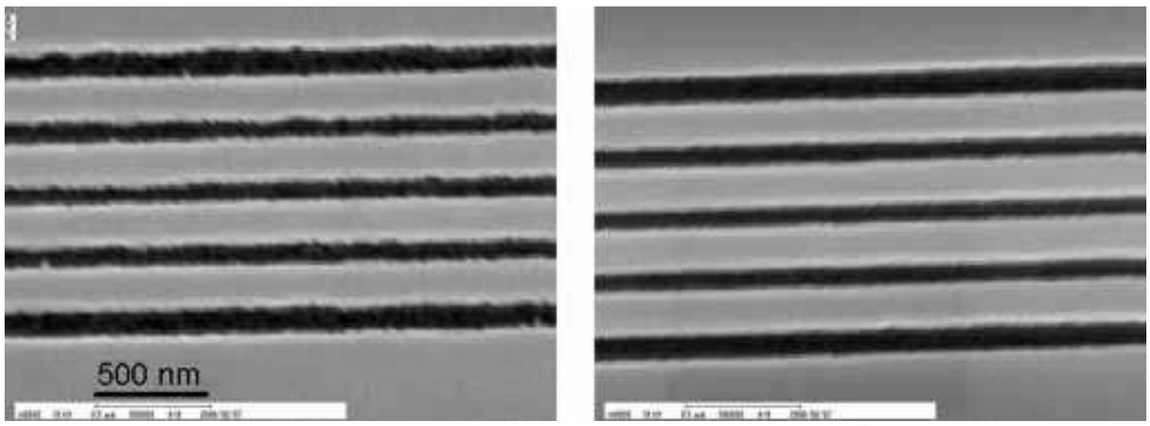

(a) (b)

Fig. 10. Comparison of LER between (a) Accuglass 512B and (b) NIMO-P0701.

The LER for Accuglass 512B was 6.77 nm, whereas the LER for NIMO-P0701 was 5.78 nm, indicating that NIMO-P0701 is better than Accuglass 512B as regards to LER. Since NIMO-P0701 has exhibited high sensitivity and low LER, it was used to image very fine patterns as shown Fig. 11.

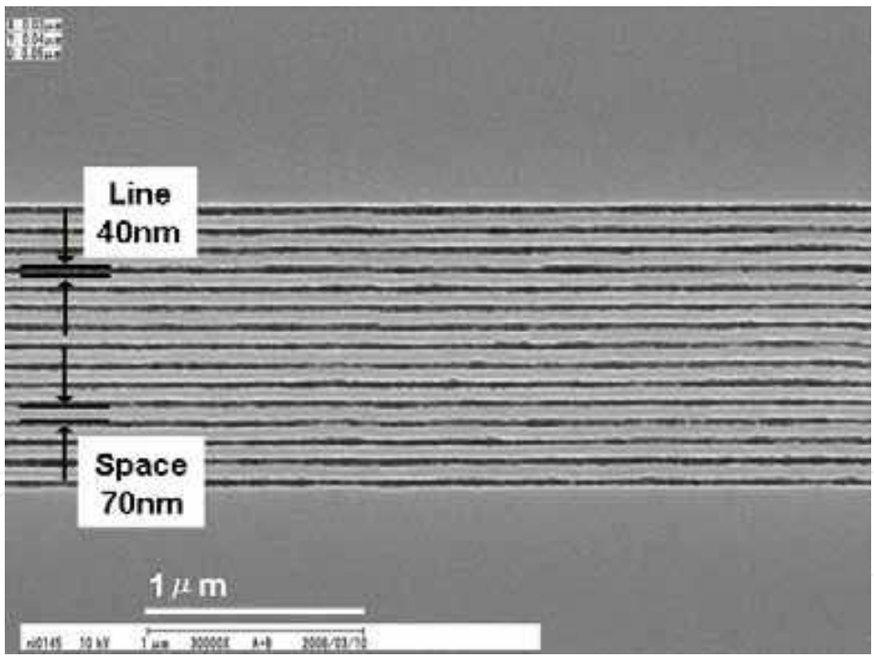

Fig. 11. The fine L&S pattern at 4 kV with NIMO-P0701.

4. Post exposure bake with the inorganic resist

A line and space (L&S) patterns, which line-width was 40 nm and space-width was 70nm, was obtained using low-acceleration-voltage EBL system with inorganic resist, NIMO-P0701 in section 3. However, the smaller space-width was not obtained with 4 kV EB because of the proximity effect. Therefore, post-exposure-bake (PEB) process was employed. Typically,

PEB was only employed for increasing the sensitivity of the resist, which has a chemically amplified material (Ocola, 2003). However, there are no chemically amplified material in NIMO-P0701, but PEB process caused the anneal effect for SOG and the proximity effect was suppressed. The experimental procedure was the same as section 2.1, except for PEB process. PEB was carried out just after EB exposure using hot plate at 200, 300, 425 ◦C for 5 minutes in air.

Fig. 12 shows the relationship between the anneal effect and PEB temperature. The acceleration voltage and EB dose were constant in 4 kV and 300 μC/cm^2, respectively. Without PEB, the line-width was 140 nm and the higher PEB temperature tended to reduce the developed line-width.

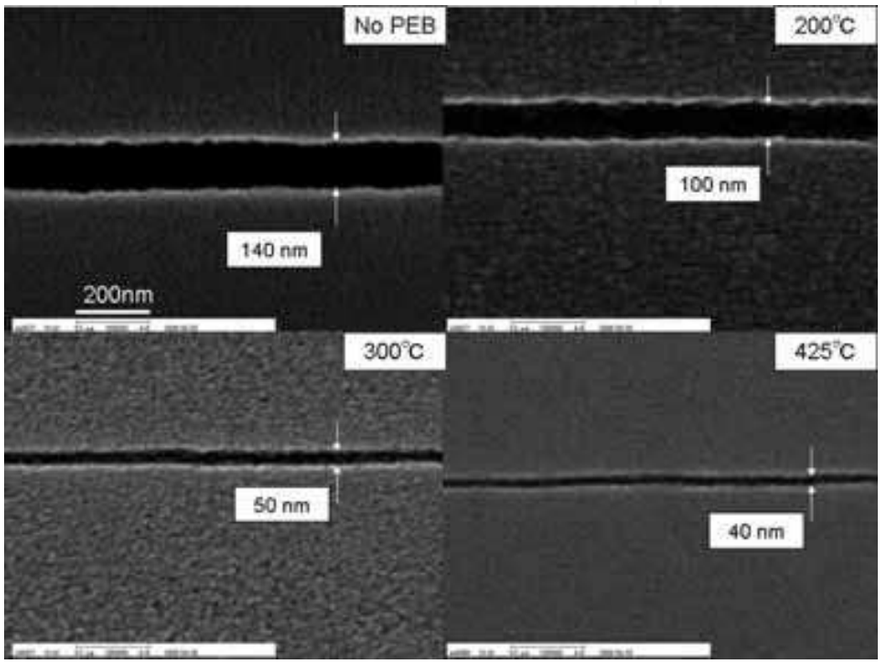

Fig. 12. The relationship between the anneal effect and PEB temperature.

Development mechanism and PEB effect is described as follows: NIMO-P0701 has chemical structures which are Si-OH, Si-CH_3 and Si-O. The main structure of NIMO-P0701 is SiO_2 and SiO_2 reacts with HF to form H_2O and H_2SiF_6, which is dissolves well into H_2O. Thus, the wetting ability between the resist surface and water dominates the etching rate of the resist. The etching rates by BHF of these chemical bonds is as follows: Si-OH > Si-CH_3 >> Si-O. On the formed resist surface, Si-CH_3 is the main structure. EB exposure accelerates the mechanism where Si-CH_3 reacts with an electron to form Si-OH. With PEB in air, Si-CH_3 changes to Si-O at the EB-unexposed area (Ahner *et al.*, 2007). Therefore, the etching rate at the un-exposed area with PEB is smaller than without PEB, result in the developed line-width reduction.

Fig. 13 shows the obtained patterns after development with or without PEB. The designed line-width is 27 nm and the space-width is 108 nm (line and space pattern, L&S). The acceleration voltage and EB dose was 2 kV and 80 μC/cm^2. Without PEB, no L&S pattern

was obtained because of the proximity effect. With PEB at 300 ◦C, in contrast, a 100 nm L&S pattern was obtained.

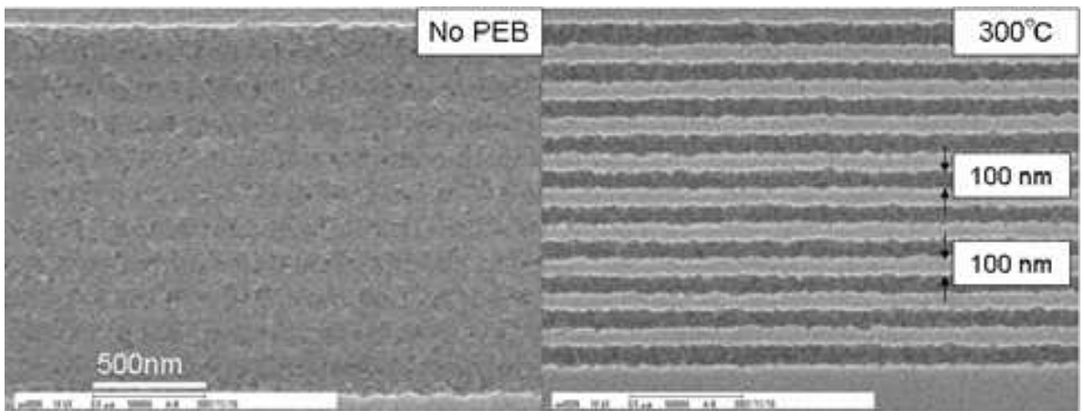

(a) (b)

Fig. 13. The obtained patterns after development (a) with or (b) without PEB.

Fig. 14 shows the cross-sections of developed L&S pattern with or without PEB at 300 ◦C, whose designed line-width and space-width were 45 nm and 270 nm, respectively. The acceleration voltage and EB dose were 4 kV and 200 μC/cm². The reverse-taper shape, which is undesirable for NIL process, was observed without PEB. However, this reverse-taper shape was prevented by PEB. These results mean that the use of PEB with an inorganic resist helps suppress the proximity effect and causes an annealing effect.

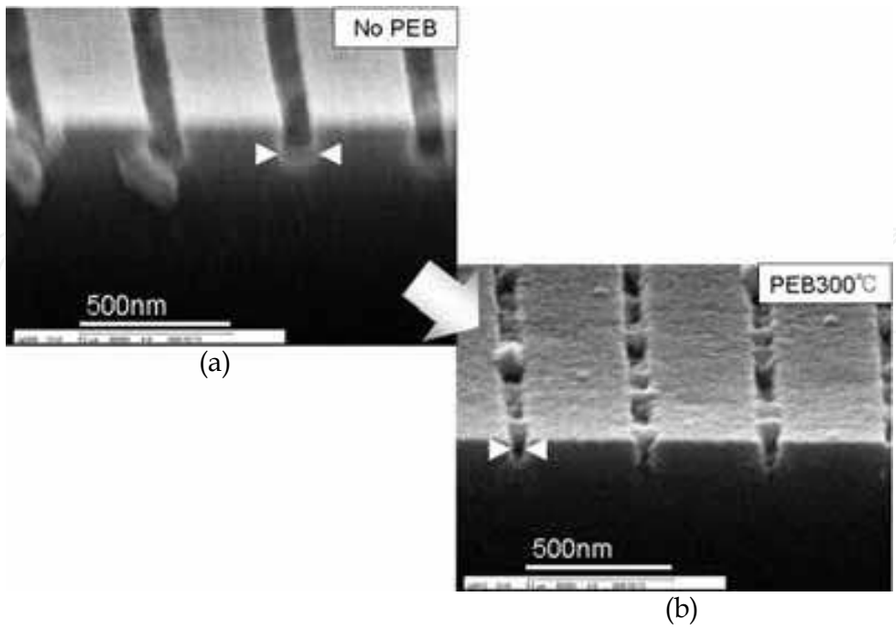

(a)

(b)

Fig. 14. the cross-sections of developed L&S pattern (a) with or (b) without PEB at 300 ◦C.

In addition, PEB is very effective in fabricating high-aspect ratio pattern in inorganic resist. In this case, thick NIMO-P0701 film (1 μm) on silicon wafer was exposed and developed to achieve the required pattern, because PEB process for the SOG suppress the proximity effect and increase the contrast. NIMO-P0701 was then written with EB. The designed line width and space width were 135 nm and 324 nm, respectively. EBL conditions were EB dose of 2500 μC/cm^2 at acceleration voltage of 30kV. Development temperature was 20 ^{o}C and development time was 1.5 min. PEB conditions were temperature of 425 ^{o}C and time of 5 min in air.

Fig. 15(a) shows the SEM image of the obtained pattern "without" PEB. This L&S pattern line, space, and depth were was 470 nm, 190 nm and 550 nm, respectively. So aspect ratio "without" PEB in the mold was 1.16. And developed resist surface was rough. In contrast, Fig. 15(b) shows the SEM image of the obtained pattern "with" PEB. This L&S pattern line, space, and depth were was 390 nm, 250 nm and 1000 nm, respectively. So aspect ratio in the case of "with" PEB in the mold was 2.59. Here the developed resist surface was smooth. An aspect ratio of "with" PEB mold was higher than that of "without" PEB, thus, influence of PEB is effective even where pattern size is of the order of submicron. Furthermore, PEB makes the surface smooth, and makes the structure vertically more anisotropic. These are some of the advantages with this type of mold.

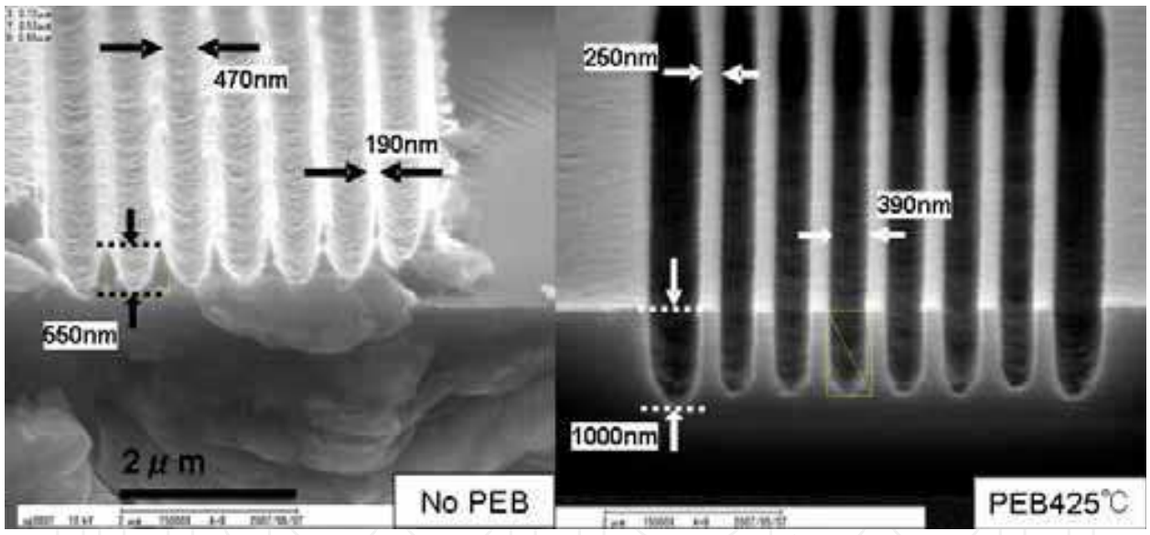

(a) (b)

Fig. 15. The SEM image of the obtained pattern (a) without or (b) with PEB.

Using the this mold with PEB, UV-NIL was carried out, similar to section 2.1. The replicated pattern from this operation is shown in Fig. 16. The obtained L&S pattern's line, space, and depth were was 280 nm, 240 nm and 940 nm, respectively. So aspect ratio of UV-NIL was 3.39. The replicated height and width were slightly smaller than mold depth and width because of volume shrinkage of photo-curable polymer by UV irradiation. As a result, using the developed EB resist layer and UV-NIL, sub-micron L&S mold were fabricated. This method does not involve dry etching which has been known to be a major cause for pattern

degradation, and is simpler than conventional LIGA and deep dry etching techniques (Ueno *et al.*, 1997).

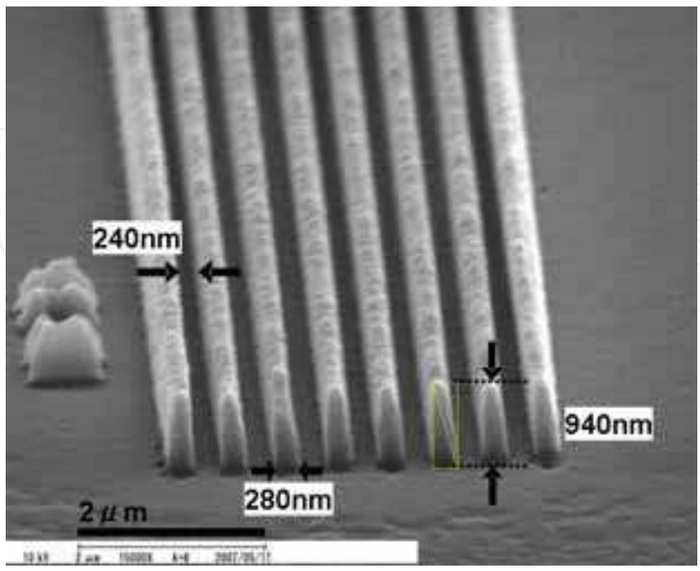

Fig. 16. The replicated pattern using high aspect ratio L&S mold.

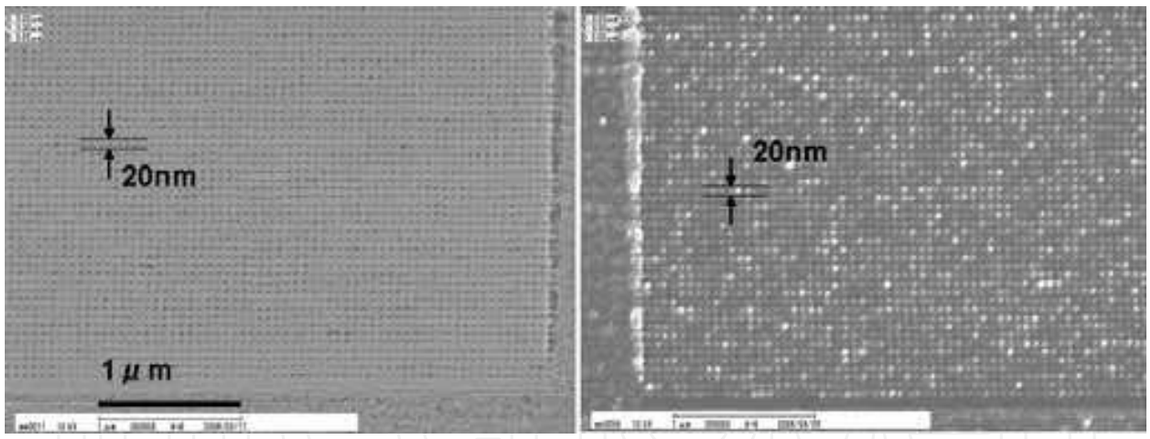

(a) (b)

Fig. 17. The SEM image of (a) 20 nm dots array pattern and (b) its replicated pattern.

Finally, nanodot array pattern was fabricated using PEB with NIMO-P0701. Nanodot array patterns will be used in patterned media and plasmonic devices of the next generation. Nanometer-scale pattern fabrication has already been applied to quantum devices optical (Fujita *et al.*, 1997). The patterned media can have a higher density of dot pattern than existing hard disk drives as a result of their ability to store magnetic information vertically. The storage density of over 1 Tb/in^2 have already been developed (Hosaka *et al.*, 2006). When these nano-meter scale structures fabricate, high acceleration voltage EBL system is normally employed as noted previously in introduction. Using our PEB process with

NIMO-P0701, however, a nanodot array pattern with 20-nm-diameter dots was obtained by 4 kV EBL (Fig. 17). This low acceleration voltage EBL system is quite inexpensive, compared to high kV one. Although the designed diameter of the nanodots was 30 nm, the areas exposed to the electron beam were shrunk to 20 nm as a result of the anneal effect of PEB at 200 ˚C. Moreover, the EB dose was 60 μC/cm² and this value is very faster than high kV EBL.

5. Conclusions

The 3D resolution of a CAV-EBL using inorganic resist has been examined. We found that the CAV-EBL can be employed to fabricate 3D NIL mold which may be in the order of just a sub-100 nm width, and can be employed to control a depth with a precision of 5 nm by simply changing the accelerating voltage by 30 V. Therefore, CAV-EBL is a suitable technique for the fabrication of binary optics element and NIL molds. Furthermore, using these molds, 3D replication patterns were obtained with UV-NIL. Thus, volume production of high value-added binary optics elements is possible using CAV-EBL and UV-NIL.
In addition, inorganic resist and post exposure bake process have been developed. These techniques help suppressing the proximity effect because of annealing effect. Consequently, developed inorganic resist (NIMO-P0701) with PEB process can fabricate high resolution and high aspect ratio NIL molds.

6. Acknowledgements

The authors thank to Mr. K. Ishikawa at TOKYO OHKA KOGYO CO., LTD, for NIMO-P0701 resist development.

7. References

Ahner, N.; Schulz, S. E.; Blaschta, F. & Rennau, M. (2008). Optical, electrical and structural properties of spin-on MSQ low-k dielectrics over a wide temperature range. *Microelectron. Eng.*, 85. pp. 2111–2113.

Chou, S. Y.; Krauss, P. R. & Renstrom, P. J. (1995). Imprint of sub-25 nm vias and trenches in polymers. *Appl. Phys. Lett.*, 67. pp. 3114-3116.

Fujita, J.; Ohnishi, Y.; Manako, S.; Ochiai, Y.; Nomura, E.; Sakamoto, T. & Matsui, S. (1997). Calixarene Electron Beam Resist for Nano-Lithography. *J Appl. Phys.*, 36. pp. 7769-7772.

Hosaka, S.; Sano, H.; Shirai M. & Sone, H. (2006). Nanosilicon dot arrays with a bit pitch and a track pitch of 25 nm formed by electron-beam drawing and reactive ion etching for 1 Tbit/in² storage. *Appl. Phys. Lett.*, 89. pp. 223131.

Ishii, K. & Matuda, T. (1992). Sub-100-nm-Scale Patterning Using a Low-Energy Electron Beam. *Jpn. J Appl. Phys.* 31.pp. L744-L746

Namatsu, H. (2001). Supercritical resist drying for isolated nanoline formation. *Jpn. Vac. Sci. Technol.*, B 19. pp.2709-2712.

Olkhovets, A. & Craighead, H. G. (1999). Low voltage electron beam lithography in PMMA. *J Vac. Sci. Technol. B*, 17. pp. 1366-1370.

Ocola, L. E. (2003). Soluble site density model for negative and positive chemically amplified resists. *J Vac. Sci. Technol. B*, 21. pp. 156-161.

Ueno, H.; Hosaka, M.; Zhang, Y.; Tabata, O.; Konishi, S. & Sugiyama, S. (1997). Study on fabrication of high aspect ratio microparts using the LIGAprocess. *Proceedings of International Symposium on Micromechatronics and Human Science*, pp. 49-54.

IntechOpen

IntechOpen

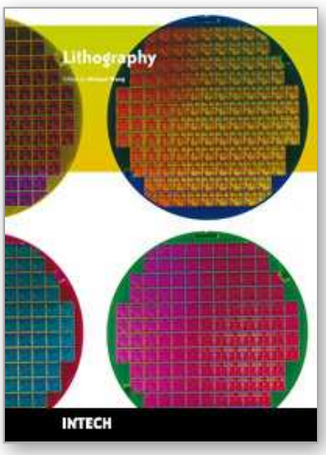

Lithography

Edited by Michael Wang

ISBN 978-953-307-064-3

Hard cover, 656 pages

Publisher InTech

Published online 01, February, 2010

Published in print edition February, 2010

Lithography, the fundamental fabrication process of semiconductor devices, plays a critical role in micro- and nano-fabrications and the revolution in high density integrated circuits. This book is the result of inspirations and contributions from many researchers worldwide. Although the inclusion of the book chapters may not be a complete representation of all lithographic arts, it does represent a good collection of contributions in this field. We hope readers will enjoy reading the book as much as we have enjoyed bringing it together. We would like to thank all contributors and authors of this book.

How to reference

In order to correctly reference this scholarly work, feel free to copy and paste the following:

Jun Taniguchi and Noriyuki Unno (2010). Three Dimensional Nanoimprint Lithography Using Inorganic Electron Beam Resist, Lithography, Michael Wang (Ed.), ISBN: 978-953-307-064-3, InTech, Available from: http://www.intechopen.com/books/lithography/three-dimensional-nanoimprint-lithography-using-inorganic-electron-beam-resist

INTECH
open science | open minds

InTech Europe
University Campus STeP Ri
Slavka Krautzeka 83/A
51000 Rijeka, Croatia
Phone: +385 (51) 770 447
Fax: +385 (51) 686 166
www.intechopen.com

InTech China
Unit 405, Office Block, Hotel Equatorial Shanghai
No.65, Yan An Road (West), Shanghai, 200040, China
中国上海市延安西路65号上海国际贵都大饭店办公楼405单元
Phone: +86-21-62489820
Fax: +86-21-62489821

© 2010 The Author(s). Licensee IntechOpen. This chapter is distributed under the terms of the Creative Commons Attribution-NonCommercial-ShareAlike-3.0 License, which permits use, distribution and reproduction for non-commercial purposes, provided the original is properly cited and derivative works building on this content are distributed under the same license.

IntechOpen

IntechOpen